Int. J. Heat Mass Transfer. Vol. 14, pp. 149–152 Pergamon Press 1971. Printed in Great Britain

SHORTER COMMUNICATIONS

CONVECTIVE HEAT TRANSFER AT GENERAL THREE-DIMENSIONAL STAGNATION POINTS

ANDRZEJ WORTMAN, HENRY ZIEGLER and GIM SOO-HOO
Northrop Corporation, Hawthorne, California, U.S.A.

(*Received* 18 *February* 1970 *and in revised form* 14 *May* 1970)

THIS note presents the results of a study of convective heat transfer in three-dimensional stagnation point flows. The properties of the gas are characterized by density inversely proportional to enthalpy, and viscosity proportional to enthalpy raised to some power. This model gas eliminates enthalpy as a parameter but retains the essential features of real gas flows.

Poots [1] presented detailed results for three-dimensional stagnation point flow of a gas with Prandtl number of unity and viscosity proportional to temperature. This work was extended to include mass transfer and nonunity Prandtl number by Libby [2] who considered shapes ranging from spheres to saddle points with adverse and favorable pressure gradients of equal magnitudes. The present investigations extend the no-mass transfer results by using more realistic variations of gas properties.

A detailed derivation of the three-dimensional stagnation point boundary-layer equations was given by Libby [2]. For convenient reference, only the transformed equations are shown here:

$$(Cf_1'')' + (f_1 + Kf_2)f_1'' + \left(\frac{\rho_e}{\rho} - f_1'^2\right) = 0, \tag{1a}$$

$$(Cf_1')' + (f_1 + Kf_2)f_2'' + K\left(\frac{\rho_e}{\rho} - f_2'^2\right) = 0, \tag{1b}$$

$$\left(\frac{C}{Pr}g'\right)' + (f_1 + Kf_2)g' = 0, \tag{1c}$$

where

a = inviscid velocity gradient in the principal direction;
$C = (\rho\mu)/(\rho\mu)_e$;
f = stream function such that $f_i' = u_i/u_{i,e}$; $i = 1, 2$;
$g = h/h_e$;
h = enthalpy;
K = ratio of transverse to principal plane pressure gradients;
Pr = Prandtl number;
z = coordinate normal to the surface;
μ = viscosity;
$\eta = \left(\frac{\rho_e a}{\mu_e}\right)^{\frac{1}{2}} \int\limits_0^{\bar{z}} \left(\frac{\rho}{\rho_e}\right) d\bar{z}$;
ρ = density.

Primes denote differentiation with respect to η. Subscripts 1 and 2 refer to the principal and transverse directions respectively. Subscript e denotes evaluation at the edge of the boundary layer; inner boundary conditions are denoted by the subscript s.

The set of governing equations (1) is subject to the boundary conditions

$$\eta = 0 \quad f_1' = 0 = f_2'; \quad f_1 = 0 = f_2; \quad g = g_s \tag{2a}$$

$$\eta \to \infty \quad f_1' \to 1{\cdot}0; \quad f_2 \to 1{\cdot}0; \quad g \to 1{\cdot}0. \tag{2b}$$

The gas properties are given by

$$\rho \alpha h^{-1}; \quad \mu \alpha h^{s_1}; \quad Pr = 0{\cdot}7. \tag{3}$$

Values of s_1 equal to 0·5, 0·7 and 1·0 were considered so that real gas properties could be approximated over a wide range of temperatures. Wall enthalpy ratios, g_s, ranging from 0·0001 to 2·0 were considered for values of the transverse pressure gradient parameter K ranging from $-1{\cdot}0$ to 1·0.

The Prandtl number was taken as constant because in most atmospheric flight problems its variation in the boundary layer is quite small (usually <5 per cent from mean value).

The method employed to compute the results presented here was developed in [3] as an application of the techniques of modern functional analysis to the general problem of multicomponent three-dimensional boundary-layer flows. Complete details of the basic theory and numerous examples of applications to several classes of problems are given in [3].

In essence, the method extends the use of iterative procedures to problems for which straightforward iteration schemes generally diverge.

The accuracy of the calculations was established by comparison with the $C = 1$, $Pr = 1$ results of Poots.

Table 1. Comparison of g'(0) results with those of Poots [2]

K	$g_s = 0$ Poots	$g_s = 0$ Present calculations	$g_s = 2.0$ Poots	$g_s = 2.0$ Present calculations
1·0	0·6989	0·6990	−0·8102	−0·8103
0·5	0·6069	0·6069	−0·7076	−0·7076
0·0	0·5067	0·5066	−0·6156	−0·6156

In addition a check was made against the $C = 1$, $Pr = 1$, $g_s = 1$ results of Davey [4], who showed that $f_2''(0) = 0$ when $K = 0{\cdot}4294$. Using 200 integration steps across the boundary layer the present calculations yielded

$$K = -0{\cdot}4293 \qquad f_2''(0) = 0{\cdot}00015$$

$$K = -0{\cdot}4294 \qquad f_2''(0) = -0{\cdot}000001.$$

Since only single precision calculations were made on the IBM 360/65 computer, no claims of six-decimal-place accuracy may be made, and the agreement is considered to be satisfactory. Only about 3 s of machine time were required for each calculation, and all the calculations were completed in a few parameter runs of several dozen cases each.

The heat transfer calculations reported here are presented in terms of a non-dimensional heat transfer parameter which is defined by the relation.

$$\lambda = \frac{C_s}{Pr_s}\frac{g'(0)}{1 - g_s}. \tag{4}$$

This particular definition is adopted because it contains most of the effects of variation of physical properties in the boundary layer. The commonly used parameter of the wall value of the ratio of Nusselt number to the square root of the Reynolds number is equal to $Pr_s\lambda/C_s^{\frac{1}{2}}$.

The appearance of minima in the λ vs. K curves shown in Figs. 1 and 2 is readily deduced from the variations of the wall shear stresses shown in Figs. 3 and 4. The explanation for the behaviour of τ_1 lies in the well-known feature of two-dimensional flows where "cold wall" boundary layers are quite insensitive to pressure gradients. The flow is dominated by the strong favorable pressure gradient in the principal plane for all values of g_s and the effect of the transverse pressure gradient decreases with increasing g_s. The effect of K on heat transfer may now be explained in terms of the known decrease of heat transfer rate with a decrease of the convection in the boundary layer. Figure 4 shows that τ_2 and hence convection decreases with decreasing K and, therefore, that $g'(0)$ decreases with decreasing K until at some negative K the velocity profiles are reversed. At this stage the transverse convection in the critical region near the wall is reversed and subsequently increases as K decreases; total convection thus increases with decreasing K, and consequently the heat transfer rate increases.

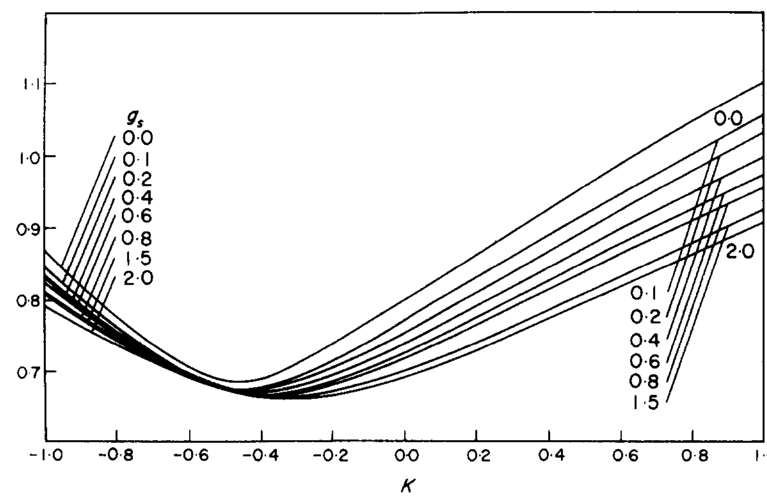

FIG. 1. Variation of the heat transfer parameter λ with K. $Pr = 0{\cdot}7$, $s_1 = 0{\cdot}5$.

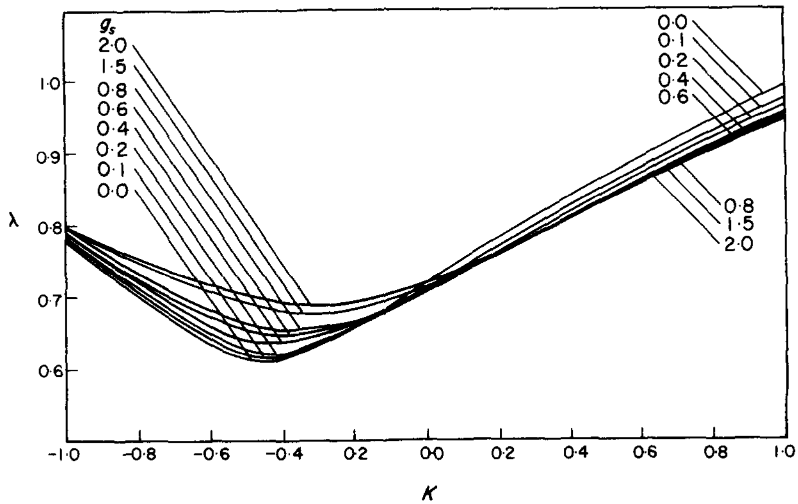

FIG. 2. Variation of the heat transfer parameter λ with K. $Pr = 0{\cdot}7, s_1 = 0{\cdot}7$.

When the heat transfer parameters are normalized by λ computed with $C_1 = 1{\cdot}0$, the effects of geometry practically disappear. In Fig. 5, where the average values of λ for all K (at a given g_s) are plotted against C_s, the maximum deviation from the average value of λ is seen to be less than 2 per cent for all values of g_s and K. When the data are approximated with a least square error curve fit, then, for $C_s \leqslant 5$,

$$\lambda^* = \lambda/\lambda_{(C=1\cdot 0)} = C_s^{0\cdot 152} \tag{5}$$

with an r.m.s. error of 3·5 per cent. In this range, the overall correlation, which includes all the effects of geometry and gas properties, is within 5 per cent of the exact results. Equation (5) is written in terms of the heat transfer parameter $\lambda_{(C=1\cdot 0)}$ calculated in [3]. For convenient reference, an abbreviated table of λ with $C = 1{\cdot}0$ is taken from [3].

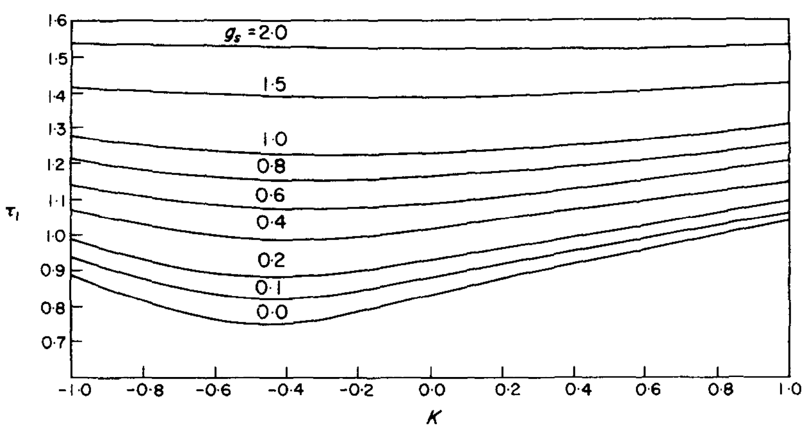

FIG. 3. Variation of the principal wall shear stress τ_1 with K. $Pr = 0{\cdot}7, s_1 = 0{\cdot}5$.

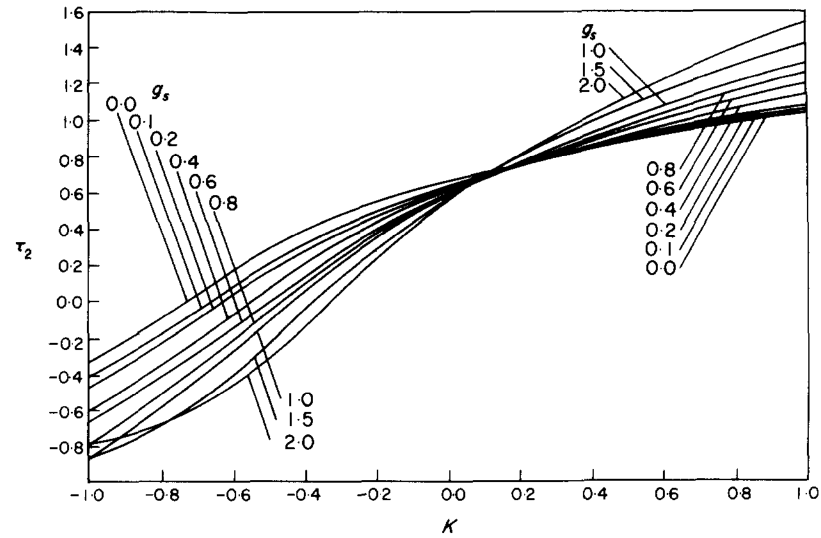

FIG. 4. Variation of the transverse wall shear stress τ_2 with K. $Pr = 0·7, s_1 = 0·5$.

Table 2. Nondimensional heat transfer parameter $\lambda, s_1 = 1·0$; Pr = 0·7

K	$g_s = h/h_e$								
	0·0001	0·01	0·1	0·2	0·4	0·6	0·8	1·5	2·0
1·0	0·8657	0·8667	0·8751	0·8854	0·9035	0·9203	0·9360	0·9842	1·0137
0·6	0·7751	0·7760	0·7843	0·7933	0·8100	0·8255	0·8485	0·8836	0·9107
0·2	0·6758	0·6768	0·6853	0·6944	0·7111	0·7265	0·7405	0·7836	0·8098
0·0	0·6233	0·6243	0·6339	0·6440	0·6623	0·6790	0·6945	0·7398	0·7671
−0·5	0·5340	0·5362	0·5547	0·5728	0·6035	0·6295	0·6525	0·7162	0·7525
−0·75	0·6041	0·6058	0·6203	0·6353	0·6623	0·6890	0·7110	0·7736	0·8003
−1·0	0·6983	0·6987	0·7130	0·6601	0·7540	0·7865	0·8075	0·8534	0·8692

REFERENCES

1. G. POOTS, Compressible laminar boundary-layer flow at a point of attachment, *J. Fluid Mech.* **22** (part 1), 197–208 (1965).
2. P. A. LIBBY, Heat and mass transfer at a general three-dimensional stagnation point, *AIAA Jl* **5**, 507–517 (1967).
3. A. WORTMAN, Mass transfer in self-similar laminar boundary-layer flows, Northrop Corporation Report, August 1969 (also Doctoral dissertation in Engineering and Applied Science at UCLA, Aug. 1969).
4. A. DAVEY, Boundary-layer flow at a saddle point of attachment, *J. Fluid Mech.* **10**, 593–610 (1961).

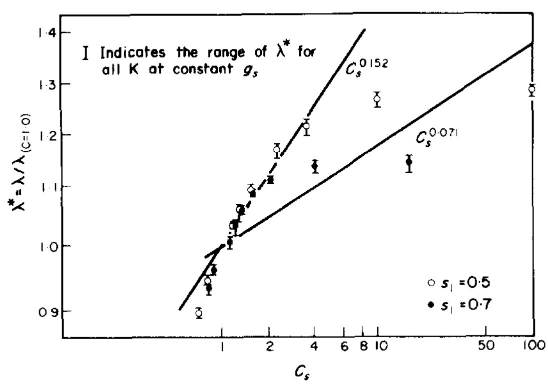

FIG. 5. Correlation of the normalized heat transfer parameter with C_s. $Pr = 0·7$.